



## Detecting changes in Arctic methane emissions: limitations of the inter-polar difference of atmospheric mole fractions

Oscar B. Dimdore-Miles<sup>1</sup>, Paul I. Palmer<sup>1</sup>, and Lori P. Bruhwiler<sup>2</sup>

<sup>1</sup>School of GeoSciences, University of Edinburgh, Edinburgh, UK

<sup>2</sup>National Oceanic and Atmospheric Administration, Earth System Research Laboratory, Boulder, Colorado, USA

*Correspondence to:* P. I. Palmer  
([paul.palmer@ed.ac.uk](mailto:paul.palmer@ed.ac.uk))

**Abstract.** We consider the utility of the annual inter-polar difference (IPD) as a metric for changes in Arctic emission of methane (CH<sub>4</sub>). The IPD has been previously defined as the difference between weighted annual means of CH<sub>4</sub> mole fraction data collected at polar stations ( $-53^\circ > \text{latitude} > 53^\circ$ ). This subtraction approach (IPD<sub>Δ</sub>) implicitly assumes that extra-polar CH<sub>4</sub> emissions arrive within the same calendar year at both poles. Using an analytic approach we show that a comprehensive description of the IPD includes terms corresponding to the atmospheric transport of air masses from lower latitudes to the polar regions. We show the importance of these transport flux terms in understanding the IPD using idealized numerical experiments with the TM5 global 3-D atmospheric chemistry transport model run from 1980 to 2010. A northern mid-latitude pulse in January 1990, which increases prior emission distributions, arrives at the Arctic with a higher mixing ratio and  $\simeq 12$  months earlier than at the Antarctic. The perturbation at the poles subsequently decays with an e-folding lifetime of  $\simeq 4$  years. A similarly timed pulse emitted from the tropics arrives with a higher value at the Antarctic  $\simeq 11$  months earlier than at the Arctic. This perturbation decays with an e-folding lifetime of  $\simeq 7$  years. These simulations demonstrate that the assumption of symmetric transport of extra-polar emissions to the poles is not realistic, resulting in considerable IPD<sub>Δ</sub> variations due to variations in emissions and atmospheric transport. We assess how well the annual IPD can detect a constant annual growth rate of Arctic emissions for three scenarios, 0.5%, 1%, and 2%, superimposed on signals from lower latitudes, including random noise. We find that it can take up to 16 years to detect the smallest prescribed trend in Arctic emissions at the 95% confidence level. Scenarios with higher, but likely unrealistic, growth in Arctic emissions are detected in less than a decade. We argue that a more reliable measurement-driven IPD metric would include data col-



lected from all latitudes, emphasizing the importance of maintaining a global monitoring network to observe decadal changes in atmospheric greenhouse gases.

## 1 Introduction

25 Atmospheric methane ( $\text{CH}_4$ ) is the second most important contributor to anthropogenic radiative forcing after carbon dioxide. Observed large-scale variations of atmospheric  $\text{CH}_4$  (Nisbet et al., 2014) have evaded a definitive explanation due to sparsity in data (Rigby et al., 2016; Turner et al., 2016; Schaefer et al., 2016; Kirschke et al., 2013; Saunio et al., 2016). Atmospheric  $\text{CH}_4$  is determined by anthropogenic and natural sources, and by loss from oxidation by the hydroxyl radical  
30 (OH) with smaller loss terms from soil microbes and oxidation by Cl. This results in an atmospheric lifetime of  $\approx 10$  years. Industrial anthropogenic  $\text{CH}_4$  sources include leakage from the production and transport of oil and gas, coal mining. Microbial anthropogenic sources include ruminants, landfills, rice cultivation, and biomass burning. The largest natural source is microbial emissions from wetlands, with smaller but significant contributions from wild ruminants, termites, wildfires, landfills, and geologic emissions (Kirschke et al., 2013; Saunio et al., 2016). Here, we focus on our  
35 ability to quantify changes in Arctic emissions using polar atmospheric mole fraction data.

Warming trends over the Arctic are approximately twice the global mean (AMAP, 2015), which is eventually expected to result in thawing of permafrost. Observational evidence shows that permafrost coverage has begun to shrink (Christensen et al., 2004; Reagan and Moridis, 2007). Arctic soils store  
40 an estimated 1700 GtC (Tarnocai et al., 2009). As the soil organic material thaws and decomposes it is expected that some fraction of this carbon will be released to the atmosphere as  $\text{CH}_4$ , depending on soil hydrology. Current understanding is that permafrost carbon will enter the atmosphere slowly over the next century, reaching a cumulative emission of 130–160 PgC (Schuur et al., 2015). If only 2% of this carbon is emitted as  $\text{CH}_4$ , annual Arctic emissions could approximately double by  
45 the end of the century from current estimates of 25 Tg  $\text{CH}_4/\text{yr}$  inferred from atmospheric inversions (AMAP, 2015). At present, using data from the current observing network there is no strong evidence to suggest large-scale changes in Arctic emissions (Sweeney et al., 2016).

The inter-polar difference (IPD) has been proposed as a sensitive indicator of changes in Arctic emissions that can be derived directly from network observations. The IPD, as previously defined  
50 (Dlugokencky et al., 2003), is the difference between weighted annual means of  $\text{CH}_4$  mole fraction data collected at polar stations ( $-53^\circ > \text{latitude} > 53^\circ$ ) such as those from the NOAA Earth System Research Laboratory (ESRL) network ([https://www.esrl.noaa.gov/gmd/dv/site/site\\_table2.php](https://www.esrl.noaa.gov/gmd/dv/site/site_table2.php)). Data from individual sites are weighted inversely by the sine of the station latitude and by the standard deviation of the data at a particular site. Hereafter, we denote this subtraction method as  $\text{IPD}_\Delta$   
55 to distinguish it from the full description of the IPD, as described below. Dlugokencky et al. (2003) reported an abrupt drop in  $\text{IPD}_\Delta$  during the early 1990s. They suggested this magnitude of change



was indicative of a 10 Tg CH<sub>4</sub>/yr reduction, which they attribute to the collapse of fossil fuel production in Russia following the 1991 breakup of the Soviet Union (Dlugokencky et al., 2011). In more recent work, Dlugokencky et al. (2011) proposed that the IPD<sub>Δ</sub> metric is potentially sensitive to changes in Arctic emissions as small as 3 Tg CH<sub>4</sub>/yr, representing a value of 10% of northern wetland emissions. However, studies have reported little or no increase in IPD<sub>Δ</sub> between 1995 and 2010 (Figure 1, Dlugokencky et al. (2011, 2003)), a period during which rising Arctic temperatures were expected to lead to an increase in emissions (Mauritsen, 2016; McGuire et al., 2017). In this work, we examine how sensitive the IPD is to changing CH<sub>4</sub> emissions by using model simulations as well as a **simple analytical approach**.

To describe the full IPD, we define the world into three contiguous regions: Arctic, background, and Antarctica (Figure 2); the inter-polar meridional length, defined from the Arctic to the Antarctic, is  $R$ . We have a local Arctic source  $L(t)$  (mass CH<sub>4</sub> per unit time) and an isolated inter-polar source  $B$  emitted at position  $r$  and time  $t$  (mass CH<sub>4</sub> per unit time). For simplicity, we assume that there is only one measurement site in the Arctic and one in Antarctica, and have neglected the transport of  $L(t)$  to the Antarctic. **The IPD in the general sense is then given by:**

$$\text{IPD}(t) = \underbrace{L(t) + \int_r^0 B(t - \tau_N, r') dr'}_{\text{Signal measured at the Arctic site}} - \underbrace{\int_r^R B(t - \tau_S, r') dr'}_{\text{Signal measured at the Antarctic site}}, \quad (1)$$

where  $\tau_N$  and  $\tau_S$  denote the time taken for source  $B$  at latitude  $r$  to reach the Arctic and Antarctic, respectively. The dummy variable  $r'$  has been introduced to avoid confusion in the integral. This relationship reduces to:

$$\text{IPD}(t) = L(t) - \int_r^0 \frac{dB}{dt} \Big|_{t-\tau_N}^{\tau_N} dr' + \int_R^r \frac{dB}{dt} \Big|_{t-\tau_S}^{\tau_S} dr'. \quad (2)$$

The purpose of this simple-minded derivation is to introduce the two independent atmospheric transport terms, which are not included in the definition of IPD<sub>Δ</sub>. A consequence of these terms, is that there are only two limiting cases in which the IPD<sub>Δ</sub> can isolate  $L(t)$ : 1) emissions from  $B$  are constant in time (second and third R.H.S. terms become zero), and 2)  $B$  arrives at both poles simultaneously (second and third R.H.S. terms cancel out). Neither case is realistic on any time scale. Even point sources are often time-dependent. The characteristic timescale for inter-hemispheric transport of an air mass is  $\simeq 1$  year (Holzer and Waugh, 2015). Using the annual IPD<sub>Δ</sub> (Dlugokencky et al., 2003) we show that only a fortuitous set of circumstances would allow this metric to isolate  $L(t)$ .

In the next section, we describe the data and methods used previously to define IPD<sub>Δ</sub>, and the model calculations we use to explore the importance of the transport flux terms in equation 2. In section 3, we report the results from our numerical experiments. We conclude in section 4.



## 2 Data and Methods

### 2.1 Observed and Model IPD<sub>Δ</sub>

90 To calculate the IPD<sub>Δ</sub>, following Dlugokencky et al. (2011), we first group together a subset of  
NOAA ESRL global monitoring measurement sites that are located  $-53^\circ > \text{latitude} > 53^\circ$  (Table 2),  
and assign them as the North and South polar regions. For each polar region we calculate mean  
biweekly mole fractions across the stations, weighted inversely by station latitude and the standard  
deviation about the biweekly mean CH<sub>4</sub> mole fraction. Biweekly values of IPD<sub>Δ</sub> are then averaged  
95 over a calendar year to determine the annual IPD<sub>Δ</sub>, which has been used in previous studies.

We use biweekly CH<sub>4</sub> values determined from measurements of discrete air samples collected in  
flasks from the NOAA Cooperative Global Air Sampling Network (NOAA CGASN). Air samples  
(flasks) are collected at the sites and analysed for CH<sub>4</sub> at NOAA ESRL in Boulder, Colorado using  
a gas chromatograph with flame 220 ionization detection. Each sample aliquot is referenced to the  
100 WMO X2004 CH<sub>4</sub> standard scale (Dlugokencky et al., 2005). Individual measurement uncertainties  
are calculated based on analytical repeatability and the uncertainty in propagating the WMO CH<sub>4</sub>  
mole fraction standard scale. Analytical repeatability has varied between 0.8 to 2.3 ppb, but averaged  
over the measurement record is approximately 2 ppb. Uncertainty in scale propagation is based on  
a comparison of discrete flask-air and continuous measurements at the MLO and BRW observato-  
105 ries and has a fixed value 0.7 ppb. These two values are added in quadrature to estimate the total  
measurement uncertainty, equivalent to a  $\simeq 68\%$  confidence interval.

Five northern and two southern polar stations (Table 2) have data that cover the period discussed in  
previous studies (approximately 1986–2010) and a weekly resolution to calculate biweekly averages.  
We impute missing data filled using a two-stage approach. We use linear interpolation to replace  
110 missing measurements from a given week and year with the average of the measurement values from  
the same week of the three preceding and subsequent years (to provide a climatological value but  
preserve long term trends in the data). If corresponding weekly measurements for the six neighboring  
years are incomplete, we use a cubic spline interpolation. We calculate the uncertainties on the  
biweekly weighted concentration means from the polar regions using the formula for the standard  
115 error.  $\sigma_{\bar{x}}$  of a weighted mean  $\mu$  (Taylor, 1997):

$$\sigma_{\bar{x}}^2(\mu) = \frac{1}{\sum_i \left( \frac{1}{\sigma_i + \sin(\phi_i)} \right)^2}, \quad (3)$$

where the denominator represents weights assigned to each station  $i$  as a function of biweekly mole  
fraction standard deviation  $\sigma_i$  and the latitude  $\phi_i$  of the station. We propagate these errors to deter-  
mine the error on the annual IPD.

120 We calculate the corresponding model IPD<sub>Δ</sub> values by sampling TM5 (described below) at the  
time and location of each NOAA ESRL observation and processing the values as describe above for  
the observations.



## 2.2 Numerical Experiments

We use the TM5 atmospheric transport model (Krol et al., 2005) to examine the transport fluxes of  
125 emissions to the polar regions (equation 2), and to determine the sensitivity of the  $IPD_{\Delta}$  to different  
emission distributions. For our experiments, we run the model using a horizontal spatial resolution  
of  $2^{\circ}$  (latitude) and  $3^{\circ}$  (longitude), forced with meteorological fields from the European Center for  
Medium Range Weather Forecast (ECMWF) ERA-Interim reanalysis. Fossil fuel and agricultural  
emission estimates are taken from the EDGAR3.2 inventory (Olivier et al., 2005) with modifications  
130 (Schwietzke et al., 2016). Natural emissions are based on the prior values used by CarbonTracker-  
 $CH_4$  (Bergamaschi et al., 2005; Bruhwiler et al., 2014). Bruhwiler et al. (2014) reported posterior  
 $CH_4$  emission estimates for high northern latitudes that were 20–30% smaller than prior values,  
which we use in our current experiments. An important consequence of our using these prior values  
is that the model  $IPD_{\Delta}$  values have a positive bias compared to values determined by  $CH_4$  mole  
135 fraction measurements.

We ran a set of targeted numerical experiments to test the sensitivity of the  $IPD_{\Delta}$  to pulsed and  
noisy variations from mid-latitude and tropical emission sources. We also considered experiments  
that included Arctic emissions with different constant growth rates and realistic variations in lower  
latitude emissions. As a control we ran a simulation with constant emissions. Appendix A includes  
140 a presentation of the time series used to calculate the  $IPD_{\Delta}$  from our experiments.

We initialized our TM5 numerical experiments from 1980 using initial conditions defined by the  
observed North-South distribution of  $CH_4$  in the early 1980s. We ran each experiment from 1980 to  
2010, and sampled mole fractions at the time and location of the network observations.

### Control Run

145 Figure 1 shows that the simulated  $IPD_{\Delta}$  for the control run is higher than observed values, as ex-  
plained above. The model  $IPD_{\Delta}$  also shows less variability than observed values, particularly in the  
early 1990s **that is attributed to a rapid decline** in fossil fuel production following the 1991 breakup  
of the Soviet Union (Dlugokencky et al., 2011). We determine the model response to changes in  
emissions (as described below) by subtracting the control run from the perturbed emissions runs.

### 150 Pulsed Emission Runs

To investigate the impact of a sustained continental-scale change in emissions on the weighted po-  
lar means and the  $IPD_{\Delta}$  metric, we run the control experiment configuration but during 1990 we  
increase emissions by an amount that is evenly distributed throughout the year. In the first pulse  
experiment, we increase existing mid-latitude emissions over the contiguous USA by 10 Tg  $CH_4$ .  
155 In the second experiment, we increase existing tropical land sources (within  $\pm 30^{\circ}$ ) by 20 Tg  $CH_4$ .



We present polar mole fraction time series produced using the control and pulsed experiments in Appendix A.

### Random Noise Emission Runs

To investigate the role of intra- and inter- variations of emission sources on the  $IPD_{\Delta}$  we re-run the two pulse experiments but superimpose standard uniform distribution noise  $\mathcal{U}(0,1)$  on the emissions. We conduct two runs of TM5: one with a noise function of amplitude 10 Tg on US emissions and another with a function of amplitude 20 Tg on tropical sources. These experiments help us to determine the observability of changes in mid-latitude and tropical sources at the poles and whether the  $IPD_{\Delta}$  can isolate  $L(t)$ .

### Arctic Emission Variation

To investigate the ability of  $IPD_{\Delta}$  to detect a constant annual growth rate of Arctic emissions, we use the control experiment configuration but in three separate experiments we increase Arctic emission by 0.5%, 1% and 2% on an annual basis. Emissions are mostly limited to summer months (June–August) when the soil surface is typically not frozen.

## 3 Results

Figure 3 summarizes the results from our pulsed emission experiments. The model response at both poles to the 1990 pulse peaks rapidly and then falls off approximately exponentially over several years. The Northern Region tracer represents the sum of  $L(t)$  and the first atmospheric transport term in equation 2, and the Southern Region tracer represents the second atmospheric transport in that equation.

Figure 3A shows that the mid-latitude pulse of 10 Tg  $CH_4$  results in a larger change at the northern polar stations (7.3 ppb peak) than at the southern polar stations (3.0 ppb peak). This reflects the longer transport time for the pulse to reach the southern stations during which time the pulse becomes more diffuse. More importantly, for the interpretation of the  $IPD_{\Delta}$  we find that the northern polar stations experience the majority of the pulse 0.96 years before the southern polar stations. After 1991 the pulse responses decay with e-folding lifetimes of 4.43 years and 8.94 years in the Northern and Southern polar stations, respectively. Figure 3C shows that the difference in pulse response at the poles decays from a maximum value in 1992 with an e-folding time of approximately 0.36 years.

Figure 3B shows that the peak of the 20 Tg  $CH_4$  tropical pulse reaches the southern polar region 0.92 years earlier than the northern polar region. This results in a larger change in southern polar  $CH_4$  mole fractions (8.3 ppb peak) compared to corresponding values over the northern polar regions. The earlier transit of the tropical pulse to the southern polar region reflects that much of the prior tropical  $CH_4$  fluxes that we perturb lie in the southern hemisphere. Responses to the tropical pulse



decay after 1992 with e-folding lifetimes of 8.65 years and 7.07 years for the northern and southern  
190 regions, respectively. The significant transport delay and disparity in responses means that an annual  
mean subtraction of northern and southern polar stations ( $IPD_{\Delta}$ ) will not remove the influence of  
the mid-latitude pulse and isolate  $L(t)$  as previously assumed.

Figure 4A shows that signal variations that we might expect from the atmospheric transport of  
intra- and inter- variations changes in emissions sources can dominate any signal that might exist in  
195 the  $IPD_{\Delta}$ . In response to noise superimposed on mid-latitude USA emissions, changes in biweekly  
 $IPD_{\Delta}$  values have a mean value of 3.0 ppb (range 6.0– -0.1 ppb). The corresponding changes in  
the annual  $IPD_{\Delta}$  has a mean value of 3.0 ppb (range 5.4–0.3 ppb). The response of the biweekly  
 $IPD_{\Delta}$  to noise on tropical emissions have a mean value of -2.8 ppb (range -12.8–5.6 ppb) and the  
corresponding response to the annual  $IPD_{\Delta}$  has a mean value of -2.7 ppb (range -4.7–0.6 ppb). These  
200 experiments show that  $IPD_{\Delta}$  is susceptible to variations in inter-polar sources.

Figure 4B shows that  $IPD_{\Delta}$  is sensitive to changes in  $L(t)$ , as expected, with a near-perfect cor-  
relation. We find only a modest response of  $IPD_{\Delta}$  to large percentage increases in Arctic emissions:  
annual increases of 0.5%, 1%, and 2% in Arctic emissions result in changes of 0.09, 0.17 and 0.35  
ppb per year in  $IPD_{\Delta}$ .  $IPD_{\Delta}$  variation that might expected from intra- and inter- variations in mid-  
205 latitude and tropical source are typically much larger than the signal associated with changes in  
 $L(t)$ . We find that the  $IPD_{\Delta}$  in the presence of a constant Arctic annual growth rate and intra- and  
inter- variations in mid-latitude and tropical emissions can detect a 0.5% annual growth rate within  
11–16 years to 95% confidence level (Weatherhead et al., 1998). Table 1 summarizes our results  
for different growth rates but generally the larger the Arctic growth rate the shorter it takes to de-  
210 tect the signal. The  $IPD_{\Delta}$  is more susceptible to variations in northern mid-latitude sources than  
tropical sources, as described above. These results represent a best-case scenario for the  $IPD_{\Delta}$ . In  
practice, there are also intra- and inter- annual variations associated with  $L(t)$  that will complicate  
the interpretation of the  $IPD_{\Delta}$  and likely increase the time necessary to detect a statistical significant  
signal.

#### 215 4 Concluding Remarks

We critically assessed the inter-polar difference (IPD) as a robust metric for changes in Arctic emis-  
sions. The IPD has been previously defined as the difference between weighted means of atmo-  
spheric  $CH_4$  time series collected in the northern and southern polar regions ( $IPD_{\Delta}$ ). A compre-  
hensive definition of the IPD includes at least two additional terms associated with atmospheric  
220 transport. Using the TM5 atmospheric transport model we highlighted the importance of these at-  
mospheric transport terms. We showed that  $IPD_{\Delta}$  has a limited capacity to isolate any change in  
Arctic emissions.



We show that an inter-polar emission arrives at one polar earlier the other pole by approximately one year, invalidating a key assumption of the  $IPD_{\Delta}$ . We also show that a small amount of noise on  
225 prior mid-latitude or tropical sources that might be expected due to intra- and inter- annual source variations is not removed in the calculation of the  $IPD_{\Delta}$ . While the  $IPD_{\Delta}$  can detect an unrealistic constant Arctic annual growth rate of emissions, any additional variation due to mid-latitude or tropical sources can delay detection of a statistical significant signal by up to 16 years.

Our study highlights the need for sustaining a spatially distributed and intercalibrated observation  
230 network for the early detection of changes in Arctic  $CH_4$  emissions. The ability to detect and quantify trends in these emissions directly from observations is attractive, but in reality we need to account for variations in extra-polar fluxes and differential atmospheric transport rates to the poles. This effectively demands the use of a model of atmospheric transport, which must be assessed using global distributed observations.

A Bayesian inference method that integrates information from prior knowledge and measurements  
235 is an ideal approach, but relies on a reliable characterization of model error and measurements that are sensitive to all major sources. Model error characterization is an ongoing process, but measurements from satellites represent new information about atmospheric  $CH_4$ . The daily global coverage of atmospheric  $CH_4$  provided by TROPOMI aboard Sentinel-5P (launched in 2017) promises  
240 to confront current understanding about Arctic emissions of  $CH_4$ . These measurements rely on reflected sunlight so they are limited by cloudy scenes and by low-light conditions during boreal winter months. Active space-borne sensors (e.g. Methane Remote Sensing Lidar Mission, MERLIN) that employ onboard lasers to make measurements of atmospheric  $CH_4$  have the potential to provide useful observations day and night and throughout the year over the Arctic. The current launch date  
245 for MERLIN in 2021. A major challenge associated with satellite observations is cross-calibrating sensors to develop self-consistent timeseries than can be used to study trends over timescales longer than the expected lifetime of a satellite instrument (nominally <5 years).

*Acknowledgements.* O.B.D. was funded by summer undergraduate project via the NERC Greenhouse gAs Uk and Global Emissions (GAUGE) project (grant NE/K002449/1). P.I.P. gratefully acknowledges his Royal Society Wolfson Research Merit Award. We thank NOAA/ESRL for the  $CH_4$  surface mole fraction data which is  
250 provided by NOAA/ESRL PSD, Boulder, Colorado, USA, from their website <http://www.esrl.noaa.gov/psd/>.





## References

- AMAP: AMAP Assessment 2015: Methane as an Arctic climate forcer, Tech. rep., Arctic Monitoring and Assessment Programme (AMAP), Oslo, Norway, 2015.
- 255 Bergamaschi, P., Krol, M., Dentener, F., Vermeulen, A., Meinhardt, F., Graul, R., Ramonet, M., Peters, W., and Dlugokencky, E.: Inverse modelling of national and European CH<sub>4</sub> emissions using the atmospheric zoom model TM5, *Atmosphere Chemistry and Physics*, 5, 2431–2460, 2005.
- Bruhwyler, L., Dlugokencky, E., Masarie, K., Ishizawa, M., Andrews, A., Miller, J., Sweeney, C., Tans, P., and Worthy, D.: CarbonTracker-CH<sub>4</sub>: an assimilation system for estimating emissions of atmospheric methane, *Atmosphere Chemistry and Physics*, 14, 8269–8293, 2014.
- 260 Christensen, T., Johansson, T., Åkerman, H., Mastepanov, M., Malmer, N., Friborg, T., Crill, P., and Svensson, B.: The role of methane in global warming: where might mitigation strategies be focused?, *Geophysical Research Letters*, 31, 2004.
- Dlugokencky, E., S.Houweling, Bruhwiler, L., Masarie, K., Lang, P., Miller, J., and Tansy, P. P.: Global atmospheric methane: budget, changes and dangers, *Geophysical Research Letters*, 30, 2003.
- 265 Dlugokencky, E., Nisbet, E., Fisher, R., and Lowry, D.: Global atmospheric methane: budget, changes and dangers, *Philosophical Transactions of the Royal Society*, 369, 2058–2072, 2011.
- Dlugokencky, E. J., Myers, R. C., Lang, P. M., Masarie, K. A., Croftwell, A. M., Thoning, K. W., Hall, B. D., Elkins, J. W., and Steele, L. P.: Conversion of NOAA atmospheric dry air CH<sub>4</sub> mole fractions to a gravimetrically prepared standard scale, *Journal of Geophysical Research: Atmospheres*, 110, n/a–n/a, doi:10.1029/2005JD006035, <http://dx.doi.org/10.1029/2005JD006035>, d18306, 2005.
- 270 Holzer, M. and Waugh, D. W.: Interhemispheric transit time distributions and path-dependent lifetimes constrained by measurements of SF<sub>6</sub>, CFCs, and CFC replacements, *Geophysical Research Letters*, 42, 4581–4589, doi:10.1002/2015GL064172, <http://dx.doi.org/10.1002/2015GL064172>, 2015GL064172, 2015.
- 275 Kirschke, S., Bousquet, P., Ciais, P., and Saunoy, M.: Three decades of global methane sources and sinks, *Nature Geoscience*, 6, 813–823, 2013.
- Krol, M., Houweling, S., Bregman, B., van den Broek, M., Segers, A., van Velthoven, P., Peters, W., Dentener, F., and Bergamaschi, P.: The two-way nested global chemistry-transport zoom model TM5: algorithm and applications, *Atmospheric Chemistry and Physics*, 5, 417–432, doi:10.5194/acp-5-417-2005, <https://www.atmos-chem-phys.net/5/417/2005/>, 2005.
- 280 Mauritsen, T.: Greenhouse warming unleashed, *Nature Geoscience*, 9, 271–272, 2016.
- McGuire, A., Kelly, B., Guy, L. S., Wiggins, H., Bruhwiler, L., Frederick, J., Huntington, H., Jackson, R., Macdonald, R., Miller, C., Olefeldt, D., Schuur, E., and Turetsky, M.: Final Report: International Workshop to Reconcile Methane Budgets in the Northern Permafrost Region., Arctic Research Consortium of the United States (ARCUS), Fairbanks, Alaska., p. 14 pages, 2017.
- 285 Nisbet, E., Dlugokencky, E., and Bousquet, P.: Methane on the Rise, Again, *Science*, 343, 493–494, 2014.
- Olivier, J., Aardenne, J. V., Dentener, F., Pagliari, V., Ganzeveld, L., and Peters, J.: Recent trends in global greenhouse gas emissions: regional trends 1970–2000 and spatial distribution of key sources in 2000, *Environmental Science*, 2, 81–99, 2005.
- 290 Reagan, M. and Moridis, G.: Oceanic gas hydrate instability and dissociation under climate change scenarios, *Geophysical Research Letters*, 34, 2283–2292, 2007.



- Rigby, M., Montzka, S., Prinn, R., White, J., Young, D., O'Doherty, S., Lunt, M., Ganesane, A., Manning, A., Simmonds, P., Salameh, P., Hart, C., Mühleg, J., Weiss, R., Fraser, P., Steele, L., Krummel, P., McCulloch, A., and Park, S.: Role of atmospheric oxidation in recent methane growth, *Proceedings of the National Academy of Sciences of the United States of America*, 114, 5373–5377, 2016.
- 295
- Saunois, M., Bousquet, P., Poulter, B., Peregon, A., and et al., P. C.: The global methane budget 2000–2012, *Earth System Science Data; Katlenburg-Lindau*, 8, 697–751, 2016.
- Schaefer, H., Fletcher, S. E. M., Veidt, C., Lassey, K. R., Brailsford, G. W., Bromley, T. M., Dlugokencky, E. J., Michel, S. E., Miller, J. B., Levin, I., Lowe, D. C., Martin, R. J., Vaughn, B. H., and White, J. W. C.: A 21st century shift from fossil-fuel to biogenic methane emissions indicated by  $^{13}\text{C}\text{H}_4$ , *Science*, doi:10.1126/science.aad2705, 2016.
- 300
- Schuur, E. A. G., McGuire, A. D., Schadel, C., Grosse, G., Harden, J. W., Hayes, D. J., Hugelius, G., Koven, C. D., Kuhry, P., Lawrence, D. M., Natali, S. M., Olefeldt, D., Romanovsky, V. E., Schaefer, K., Turetsky, M. R., Treat, C. C., and Vonk, J. E.: Climate change and the permafrost carbon feedback, *Nature*, 520, 171–179, doi:10.1038/nature14338, 2015.
- 305
- Schwietzke, S., Sherwood, O. A., Bruhwiler, L. M. P., Miller, J. B., Etiope, G., Dlugokencky, E. J., Michel, S. E., Arling, V. A., Vaughn, B. H., White, J. W. C., and Tans, P. P.: Upward revision of global fossil fuel methane emissions based on isotope database, *Nature*, 538, 88–91, doi:doi:10.1038/nature19797, 2016.
- Sweeney, C., Dlugokencky, E., Miller, C. E., Wofsy, S., Karion, A., Dinardo, S., Chang, R. Y.-W., Miller, J. B., Bruhwiler, L., Crotwell, A. M., Newberger, T., McKain, K., Stone, R. S., Wolter, S. E., Lang, P. E., and Tans, P.: No significant increase in long-term  $\text{CH}_4$  emissions on North Slope of Alaska despite significant increase in air temperature, *Geophysical Research Letters*, 43, 6604–6611, doi:10.1002/2016GL069292, <http://dx.doi.org/10.1002/2016GL069292>, 2016GL069292, 2016.
- 310
- Tarnocai, C., Canadell, J. G., Schuur, E. A. G., Kuhry, P., Mazhitova, G., and Zimov, S.: Soil organic carbon pools in the northern circumpolar permafrost region, *Global Biogeochemical Cycles*, 23, n/a–n/a, doi:10.1029/2008GB003327, <http://dx.doi.org/10.1029/2008GB003327>, gB2023, 2009.
- Taylor, J.: *Introduction To Error Analysis: The Study of Uncertainties in Physical Measurements*, University Science Books, 2nd edn., 1997.
- Turner, A., Frankenberger, C., Wennberg, P., and Jacob, D.: Ambiguity in the causes for decadal trends in atmospheric methane and hydroxyl, *Proceedings of the National Academy of Sciences of the United States of America*, 114, 5367–5372, 2016.
- 320
- Weatherhead, E. C., Reinsel, G. C., Tiao, G. C., Meng, X.-L., Choi, D., Cheang, W.-K., Keller, T., DeLuisi, J., Wuebbles, D. J., Kerr, J. B., Miller, A. J., Oltmans, S. J., and Frederick, J. E.: Factors affecting the detection of trends: Statistical considerations and applications to environmental data, *Journal of Geophysical Research: Atmospheres*, 103, 17 149–17 161, 1998.
- 325

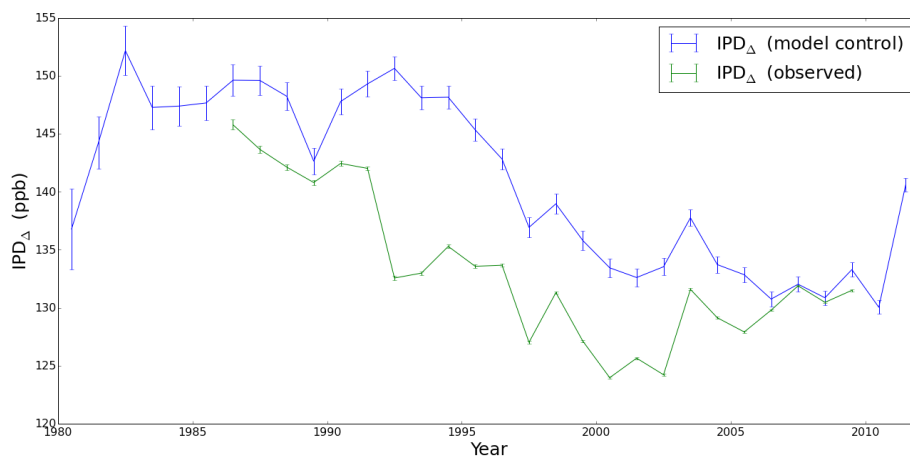


**Figure 1.** Annual mean  $IPD_{\Delta}$  values (ppb) determined by NOAA ESRL and TM5 model atmospheric  $CH_4$  mole fractions using data collected at seven geographical locations (Table 2). Vertical bars denote the one standard deviation associated with the annual mean.

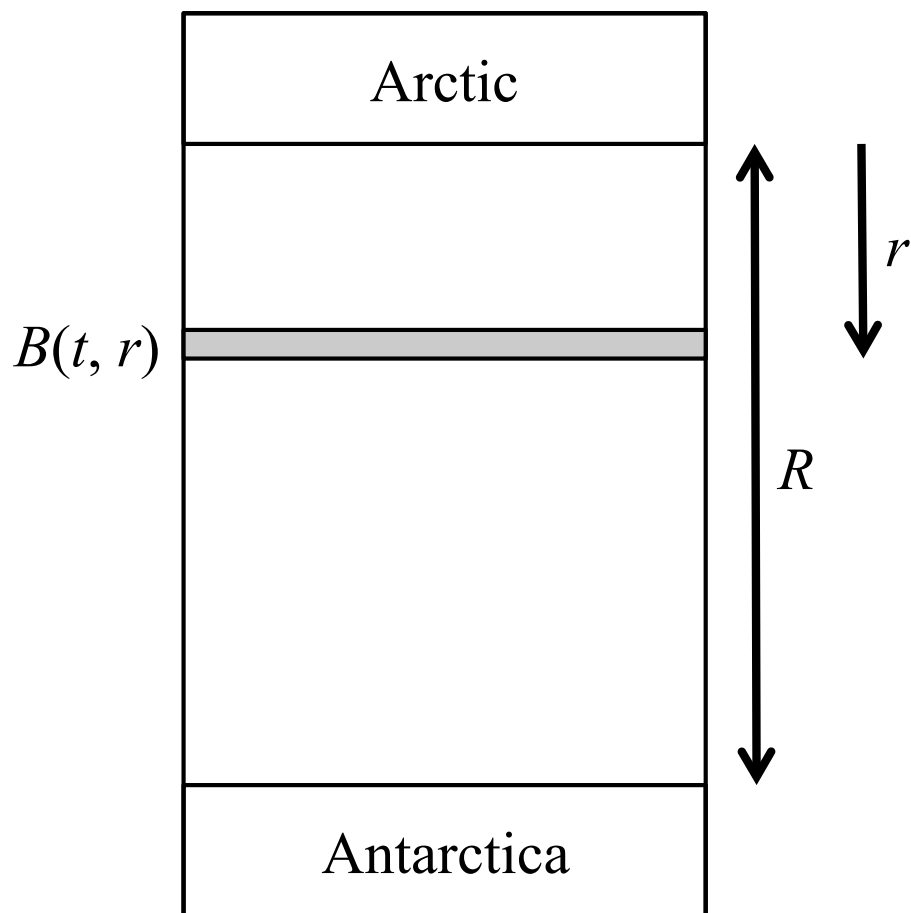


**Figure 2.** Schematic to describe how an inter-polar source  $B(t, r)$  would be viewed at measurement sites in the Arctic and Antarctic.

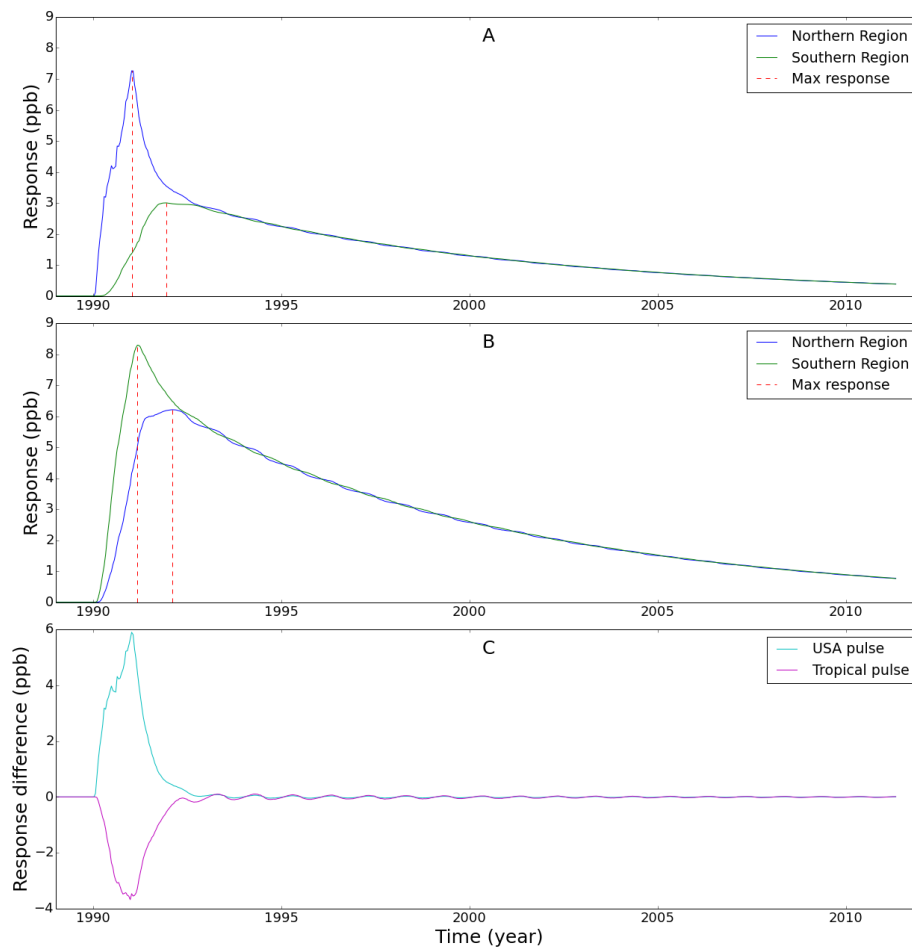


**Figure 3.** The model response of atmospheric CH<sub>4</sub> mole fraction sampled at northern and southern polar regions to a pulsed emission at (A) mid-latitude USA and (B) the tropics. Panel C shows the IPD response to these mid-latitude and tropical perturbations. In the interest of clarity, we omit error bars from the plots. Vertical red dashed lines denote the peak response time for each polar region.

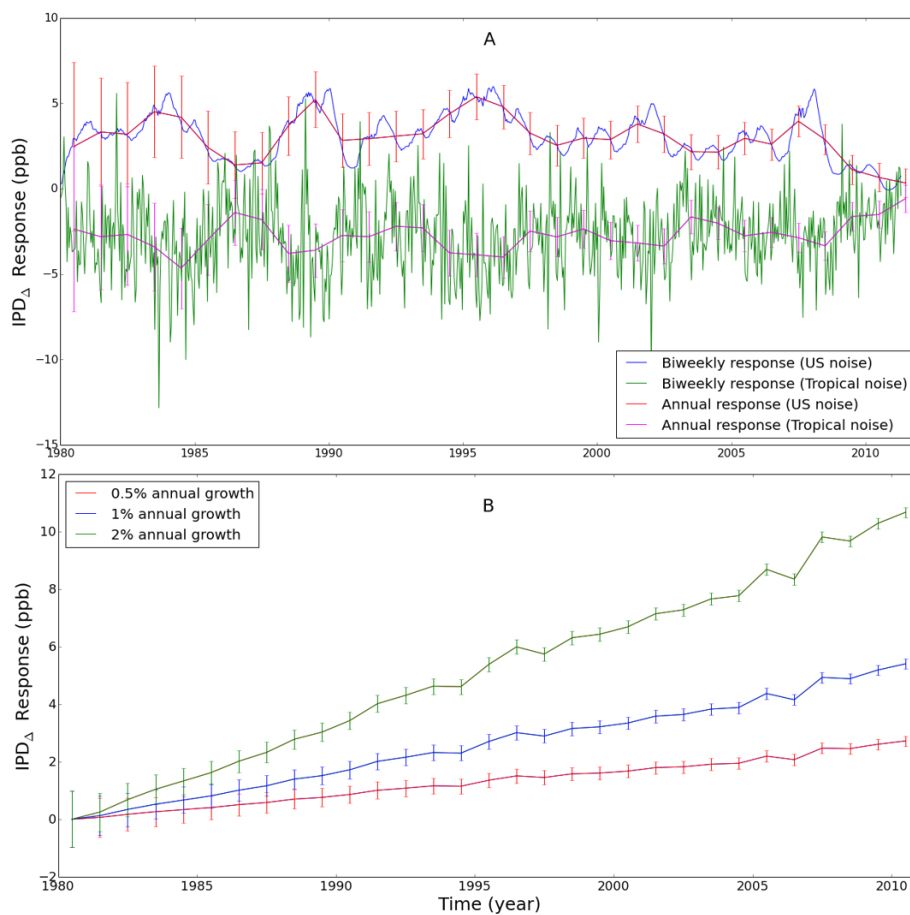


**Figure 4.** (A) Biweekly and annual model response of the IPD<sub>Δ</sub> to changes in standard uniform distribution of random noise on prior mid-latitude USA and tropical emissions. (B) annual mean response of IPD<sub>Δ</sub> to constant growth of Arctic emissions. Vertical lines denote uncertainties on responses.

**Table 1.** Details of the polar station used to calculate the  $IPD_{\Delta}$ .

Station Name	Abbreviation	Latitude (°)	Longitude (°)	Altitude (m)
Barrow, Alaska	BRW	71.32	-156.61	11.0
Alert, Canada	ALT	82.45	-62.51	190.0
Cold Bay, Alaska	CBA	55.21	-162.72	21.3
Ocean Station M, Norway	STM	66.00	2.00	0.0
Shemya Island, Alaska	SHM	52.71	174.13	23.0
South Pole, Antarctica	SPO	-89.98	-24.80	2810.0
Palmer Station, Antarctica	PSA	-64.92	-64.00	10.0



**Table 2.** Number of years required to detect a statistically significant trend in Arctic emissions in the presence of inter-polar emission variations.

Arctic Emission Annual Growth rate	Inter-polar Variation	Years to detect trend in $IPD_{\Delta}$
0.5%	USA (10 Tg amplitude random noise)	16.3
	Tropics (20 Tg amplitude random noise)	10.9
1.0%	USA (10 Tg amplitude random noise)	10.3
	Tropics (20 Tg amplitude random noise)	6.9
2.0%	USA (10 Tg amplitude random noise)	6.5
	Tropics (20 Tg amplitude random noise)	4.3





## Appendix A: IPD plots

For completeness, here we include the plots that complement the analysis reported in the main text. Figure 5 shows the model  $\text{CH}_4$  mole fraction corresponding to the weighted mean values at northern and southern polar region used to calculate the  $\text{IPD}_\Delta$  in the control and pulsed experiments using the TM5. Figure 6 shows values  
330 of the annual mean  $\text{IPD}_\Delta$  corresponding to our numerical experiments.

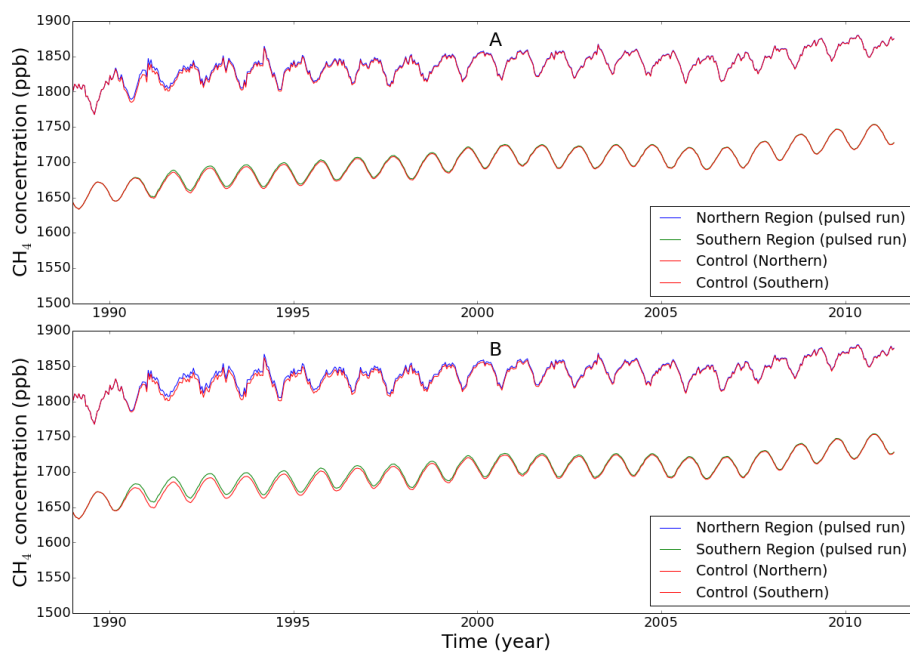


**Figure 5.** TM5 model  $\text{CH}_4$  mole fractions (ppb) sampled at polar regions (Table 2) and weighted inversely by station latitude and standard deviation of the data at that site (see main text). Panel A shows the response of a 10 Tg pulse over mid-latitude USA in 1990 over the northern and southern pole. Panel B shows the response of a 20 Tg pulse over the tropics during 1990.

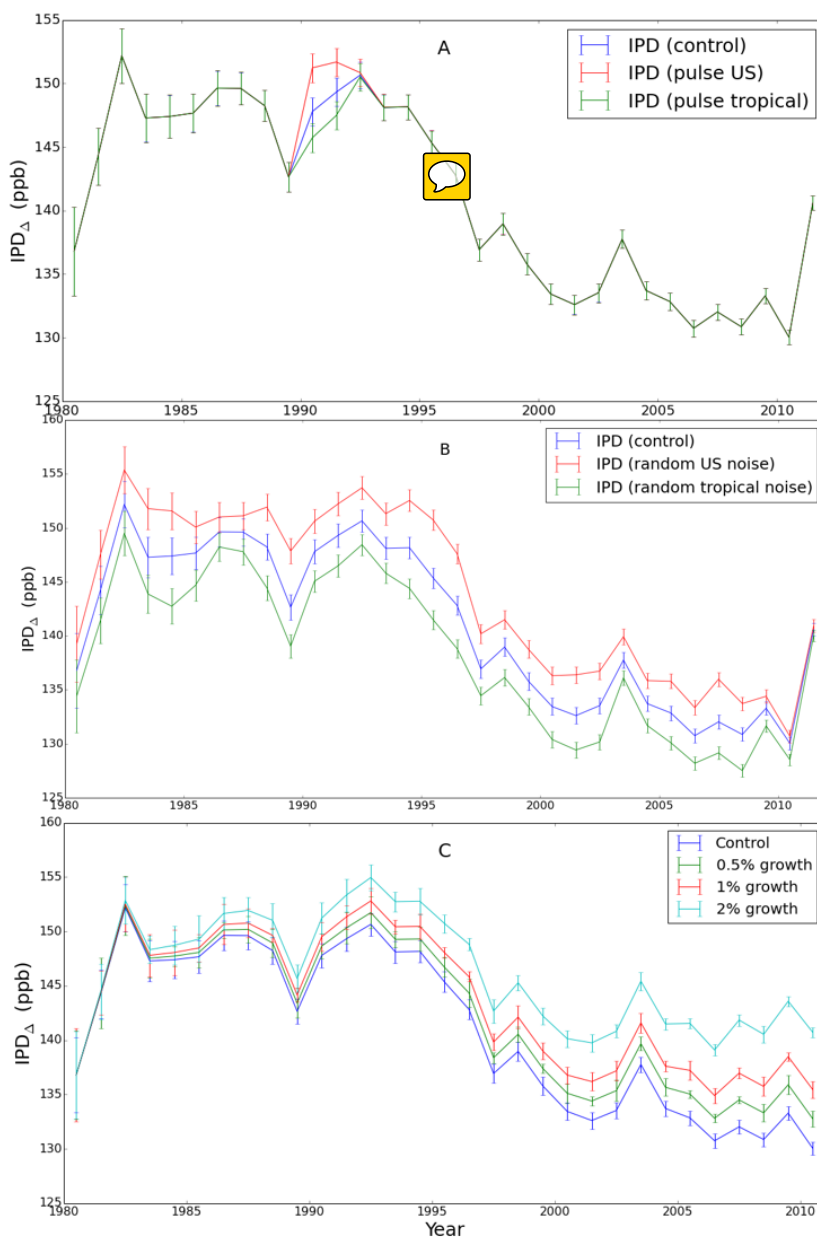


**Figure 6.** The model IPD $\Delta$  corresponding to the control and all the sensitivity experiments described in the main text.